ISSN 1392 - 1207. MECHANIKA. 2007. Nr.1(63)

Slider-link driven compressor (II). Simulation results

V. Dagilis*, L. Vaitkus, D. Kirejchick*****

**Kaunas University of Technology, K. Donelaičio g. 20, 44239 Kaunas, Lithuania, E-mail: Vytautas.Dagilis@ktu.lt*

***Kaunas University of Technology, K. Donelaičio g. 20, 44239 Kaunas, Lithuania, E-mail: Liutauras.Vaitkus@ktu.lt*

****JSC "Atlant", Nakonechnikov 50, 225320 Baranovichi, Republic of Byelorussia, E-mail: bsz@atlant.belpak.brest.by*

1. Solution of crankshaft's equation of rotating motion

The mathematical model of slider – link driven compressor, presented in the first part of the article, can be used for evaluation of unbalanced inertia forces, vibrations and losses due to friction. Possible alternatives of problem definition, solution algorithms, simulation examples and some results are presented in this article.

Rotary behavior of the crankshaft is subject to the equation of rotating motion of the crankshaft Eq. (35) in [1]. The right term of the equation represents the driving torque and loads that are functions of φ, $\dot{\varphi}$ and $\ddot{\varphi}$. The equation can be arranged to the expression $\ddot{\varphi} = f(\ddot{\varphi},\dot{\varphi},\varphi,t)$. The usual approach with hydrodynamic bearings is to assume that eccentricity ratio of the shaft center is lower than 1%, calculating friction coefficients for the bearings according to the Petroff law. In our case, however, the bearings are heavily loaded, thus the equation in which eccentricity in the bearing is taken into account was chosen for the model. The following system of four nonlinear equations is solved at every step of numeric integration

$$\left.\begin{aligned}
&\ddot{\varphi} + (\gamma_4 + I_z)^{-1}\left[\gamma_5\dot{\varphi}^2 - M_v + M_k + M_a + M_b + \right.\\
&\qquad \left. + M_s + M_t + \gamma_6\left(F_g - F_{FG}\right)\right] = 0\\
&\left(\Phi_p\right)_k - \left(c_k/r_k\right)^2/\left(\eta\dot{\varphi}\right)\times F_k/\left(2l_k r_k\right) = 0\\
&\left(\Phi_p\right)_a - \left(c_r/r_r\right)^2/\left(\eta\dot{\varphi}\right)\times F_a/\left(2l_a r_r\right) = 0\\
&\left(\Phi_p\right)_b - \left(c_r/r_r\right)^2/\left(\eta\dot{\varphi}\right)\times F_b/\left(2l_b r_r\right) = 0
\end{aligned}\right\} \qquad (1)$$

where c_k, c_r are radial clearances of crankpin and crankshaft bearings ; l_k, l_a, l_b are lengths of crankpin and crankshaft bearings (upper and lower).

The first equation of system (1) is obtained from Eq. (35) in [1], the next three equations are obtained from Eq. (22) in [1] for the corresponding bearings. In the system of equations the independent variables are angular velocity $\ddot{\varphi}$ and eccentricity ratios in the bearings ε_k, ε_a and ε_b. In the first equation of the system frictional moments $M_k = f(l_k/d_k,\varepsilon_k)$; $M_a = f(l_a/d_r,\varepsilon_a)$; $M_b = f(l_b/d_r,\varepsilon_b)$ are calculated according to Eq. (23) in [1] and friction coefficients are obtained from the Eq. (21) in [1]. Dimensionless coefficients Φ_P and Φ_T (Fig. 1, 2) were obtained by interpolation of classical reference tables.

Motor torque is the function of angular velocity. Fig. 3 shows the experimentally measured motor torque characteristic for the motor with nominal capacity 120 W.

Gas pressure in the cylinder required for the calculation of gas force is calculated using the mathematical model described in [2, 3]. The relationship $p_c = f(\varphi)$ is obtained as a sequence of discrete values. Intermediate values are calculated using the spline interpolation.

Before the equation of rotating motion of the crankshaft can be solved, mass characteristics of moving parts must be found. For solving equation of vibrations (42) or Eq. (43) in [1] the mass characteristic of the whole compressor are also required. Since the model is intended to be used by engineers at early stage of compressor design, calculation of the mass properties would be preferable over the experimental methods of their determination. However, the whole compressor is heterogeneous body of complicated shape and calculation of its mass characteristics is problematic. The gravity center and inertia moments of the compressor with the piston at the upper dead center were measured by applying the principle of rigid pendulum with measurement accuracy of about 2%. To simplify mathematical model, mass characteristics of the whole compressor were assumed constant. The mass characteristics of moving parts were determined using 3D modeling in Solid Works. Models of the piston and the crankshaft with different values of stroke and diameter were built, the intermediate values of mass characteristics were obtained by interpolation. Model of the piston was built assuming the distance from the axis of rotation to the end of the cylinder constant (as for current design of analyzed compressor). While building the 3D models attention must be focused on proper positioning of coordinate axes, which must coincide with the coordinates used in the model.

The first equation of system (1) contains variables γ_4, γ_5 and γ_6, defined in Eq. (34) in [1]. These variables contain $\delta_1 - \delta_5$, defined in Eq. (5) in [1]. However, values of the variables cannot be determined before the system (1) is solved, since directions of forces F_{GN1}, F_{GN2} and F_{BN} are unknown. The initial values of δ_3, δ_4 and δ_5 are assumed, and the assumption is verified after the forces are found from the Eqs. (11) in [1]. If the directions of the calculated forces do not coincide with the assumed directions, the assumption is changed and calculations repeated. The following algorithm is used at every step:

1. Initial values of the variables δ_3, δ_4 and δ_5 are set.
2. The system of nonlinear Eqs. (1) is being solved numerically; values of $\ddot{\varphi}$, ε_k, ε_a and ε_b are found.
3. Using the Eq. (11) in [1], the constraint forces F_{GN1}, F_{GN2} and F_{BN} are calculated.
4. Variables δ_3, δ_4 and δ_5 are being found using the Eq. (6) in [1]. If the obtained values do not coincide with the initially set values, different initial values

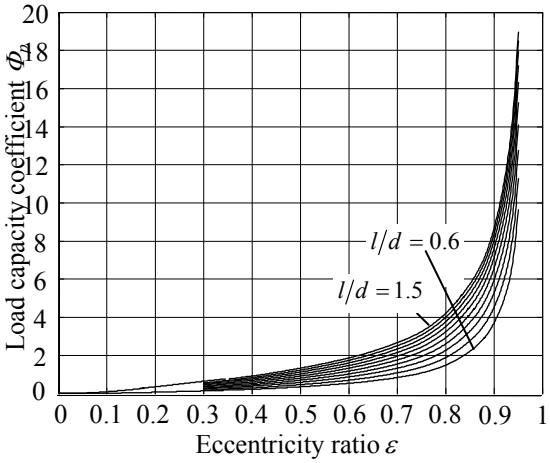

Fig. 1 Load capacity coefficient Φ_P subject to eccentricity ratio ε and l/d ratio (l/d step 0.1)

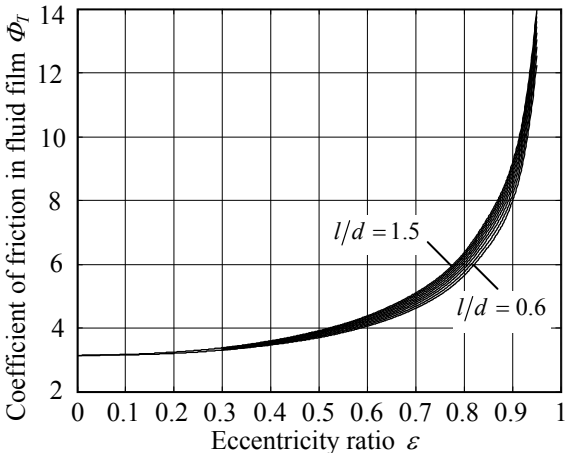

Fig. 2 Coefficient of friction in fluid film Φ_T subject to eccentricity ratio ε and l/d ratio (l/d step 0.1)

must be set and calculations repeated from the step 1.

The values of variables δ_3, δ_4 and δ_5 from the last successful iteration are stored and used as initial setting for the consequent step. Then initial settings will require adjustment only at the points, where constraint forces F_{GN1}, F_{GN2} and F_{BN} change their direction.

2 Simulation results

There are a few possible problem definitions for the calculation of crankshaft dynamic behaviour. If the values of friction coefficients μ_c, μ_s are available, the following boundary condition must be satisfied $(d\varphi/dt)_0 = (d\varphi/dt)_{2\pi}$, where $(d\varphi/dt)_0$ is initial crankshaft speed ($\varphi = 0$; $t = 0$); $(d\varphi/dt)_{2\pi}$ is final crankshaft's speed ($\varphi = 2\pi$; $t = \tau$, where τ is the period of rotation). In such a case nonlinear shooting method can be applied, in which boundary value problem is replaced by sequence of initial value problems. Such conditions are used when rotation period cannot be experimentally determined, e.g. at the initial stage of new compressor design.

When friction coefficients μ_c, μ_s are not set, additional information is required, e.g. rotation period τ.

Friction coefficients can be assumed equal $\mu_c = \mu_s$, and the problem is presented as the following system

$$\begin{cases} (d\varphi/dt)_0 = (d\varphi/dt)_{2\pi} \\ t_{2\pi} = t_g \end{cases} \quad (2)$$

where t_g is given rotation period and $t_{2\pi}$ is rotation period, obtained by solving differential equation (initial value problem). Nonlinear shooting method should be applied for solving the problem, with crankshaft speed $(d\varphi/dt)_0$ and friction coefficient $\mu = \mu_c = \mu_s$ as independent variables. Such problem definition is suitable for model verification and validation, since rotational frequency can be determined with simple experiment.

An experimental compressor, based on CKH-130H5 (from "Atlant", Byelorussia) was chosen for model verification. Mechanical constants of the compressor are presented in Table 1.

The Fig. 5 shows the rotary behavior of the crankshaft, calculated for evaporation temperature $t_0 = -25\,^{\circ}\mathrm{C}$ and condensing temperature $t_c = 40\,^{\circ}\mathrm{C}$. The calculated periodic time for one revolution of the crankshaft is $\tau = 20.538$ ms. The crankshaft speed $\dot{\varphi}$ fluctuates from

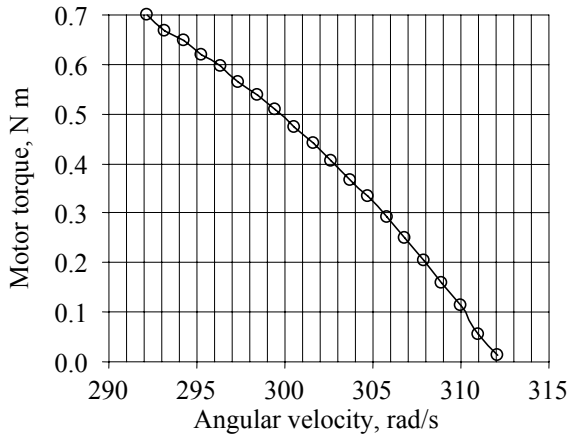

Fig. 3 Measured motor torque characteristics for the motor with nominal capacity 120 W

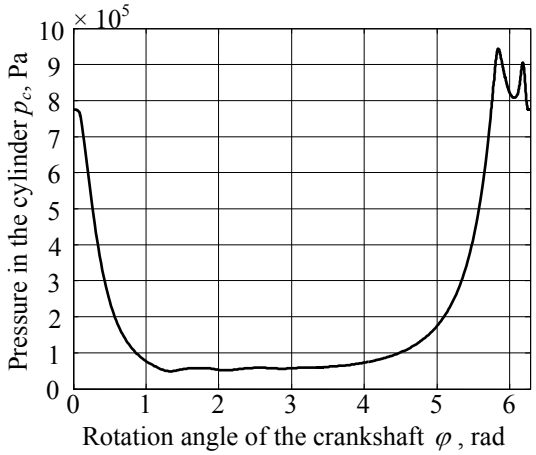

Fig. 4 Calculated pressure in the cylinder p_c; $t_o = -25$ ºC, $t_c = 55$ ºC, refrigerant R600a

Table 1

Mechanical constants

c_k	$1.0\cdot10^{-5}$ m	h_{w1}	$5.0\cdot10^{-3}$ m	l_k	$1.6\cdot10^{-2}$ m	R_t	$1.25\cdot10^{-2}$ m	z_p	$2.85\cdot10^{-2}$ m
c_p	$6.5\cdot10^{-6}$ m	h_{w2}	0 m	L_p	$4.74\cdot10^{-2}$ m	r_t	$9.5\cdot10^{-3}$ m	z_s	$9.2\cdot10^{-2}$ m
c_r	$1.0\cdot10^{-5}$ m	$J_{x'z}$	$2.4\cdot10^{-6}$ kg m^2	m_p	$9.47\cdot10^{-2}$ kg	R	$9\cdot10^{-3}$ m	μ_c	0.04
D	$2.6\cdot10^{-2}$ m	J_z	$4.07\cdot10^{-4}$ kg m^2	m_r	1.0275 kg	x_c	$8.5\cdot10^{-3}$ m	μ_s	0.04
D_s	$2.1\cdot10^{-2}$ m	l_a	$1.2\cdot10^{-2}$ m	m_s	$2.82\cdot10^{-2}$ kg	z_b	$3.2\cdot10^{-2}$ m	μ_t	$9.5\cdot10^{-2}$ m
e	$2.0\cdot10^{-3}$ m	l_b	$1.2\cdot10^{-2}$ m	r_k	$7.0\cdot10^{-3}$ m	z_{w1}	–0.0135 m	η	$3.8\cdot10^{-3}$ Pa·s
e_{cr}	$3.05\cdot10^{-4}$ m	L_c	$3.4\cdot10^{-2}$ m	r_r	$9.0\cdot10^{-3}$ m	z_{w2}	$4.45\cdot10^{-2}$ m		

302.26 to 309.24 rad/s, and hence the speed variation is about 2.28 %. The angular acceleration $\ddot{\varphi}$ fluctuates from -2484 rad/s^2 to 1269 rad/s^2 and the fluctuating *p-p* value is about 3750 rad/s^2. The sharp peak of $\ddot{\varphi}$ at the time 18.7 ms corresponds well to the first peak of p_c shown in Fig 4.

Fig. 6 shows experimental results and corresponding calculated values of crankshaft speed (revolutions per minute) subject to evaporation temperature t_0 $\left(t_c = 55\,^{\circ}\mathrm{C}\right)$. Calculated results simulate precisely the measured values – the difference is less than 0.2%. Friction coefficients assumed equal $\mu_c = \mu_s = 0.04$ which is reasonable for boundary lubrication. The same values of friction coefficients were assumed in [4] for friction in rotary compressor. In [5] also Coulumb type friction was used to describe friction at the vane tip and vane sides of rotary compressor, but lower values of friction coefficients were assigned (0.02). However, as recognized by authors, the calculated power input was always underpredicted. In [6] the connecting rod driven reciprocating compressor was analyzed. Authors considered friction coefficient between the cylinder and piston equal to 0.05 (friction in a fluid film was not taken into account separately). The rest friction coefficients considered equal to 0.02 (the latter value seems a bit overestimated, since the friction pairs should be under hydrodynamic lubrication).

Fig. 7 and Fig. 8 show reactions and friction forces, exerted on the piston. Most of the time the center line of the piston does tilt in clockwise or counterclockwise directions. Only for the short period the piston does not tilt and is pressed to the right side of the cylinder. This may be important for evaluating volumetric losses because of the leak between compressors piston and cylinder, since such a position occurs in the discharge process, when pressure difference is the highest. According to [3], when the piston does tilt in clockwise or counterclokwise direction, the gas flow through the clearance 1.65 times exceeds the flow through the regular clearance (when centrelines of the cylinder and the piston coincide). When the piston is pressed to the wall of the cylinder, the gas flow will be 2 times as big, as for the case of regular clearance.

The Fig. 7 also shows the combinations of δ_3, δ_4 and δ_5, occurring during normal operation of the compressor. The following sets of corresponding variables do occur (-1, 1, 1), (1, -1, 1), (-1, 1, -1), (-1, -1, 1). To speed up the calculations, these sets should be verified first.

Fig. 9 shows loads of the bearings, and Fig. 10 shows calculated eccentricity ratios of the bearings. Selection of 3D model for the crankshaft is reasonable, since for the 2D model of the crankshaft the calculated loads F_a and F_b would have been unreasonably lowered almost 3 times. Fig. 10 also proves that the use of relationships for unloaded bearings for the calculation of friction coefficients would have not look reasonable since the bearings are heavily loaded (eccentricity ratios reaches 0.8). However the choice of the equation for friction coefficients calculation deserves some discussion.

We tried to calculate frictional moments in bearings using both Eq. (20) in [1] and Eq. (21) in [1] (see Fig. 13).

In Eq. (20) in [1] eccentricity in the bearings is not taken into account, thus Eq. (21) in [1] should give more accurate results. However, for optimization of the bearings even Eq. (21) in [1] may be not accurate enough. First of all, the coefficients Φ_T and Φ_P are obtained for

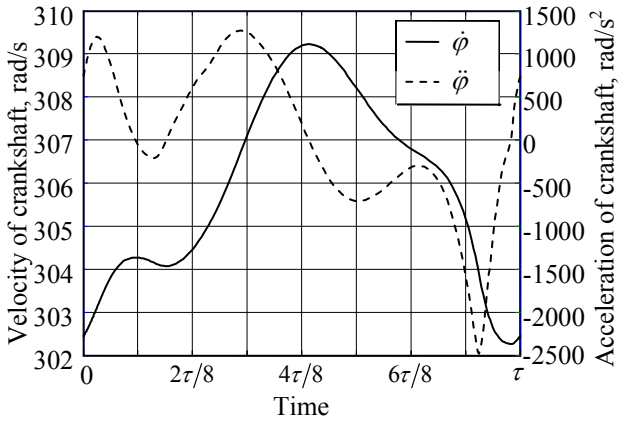

Fig. 5 Rotary behaviour of the crankshaft; $\dot{\varphi}, \ddot{\varphi}$ - velocity and acceleration of the crankshaft; $\tau = 20.538$ ms

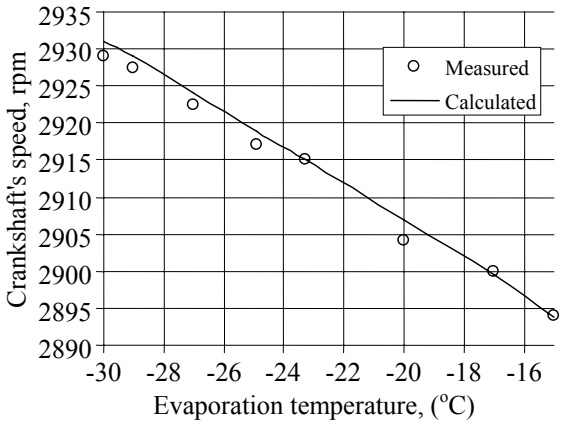

Fig. 6 Crankshafts speed subject to evaporation temperature; condensing temperature 55ºC

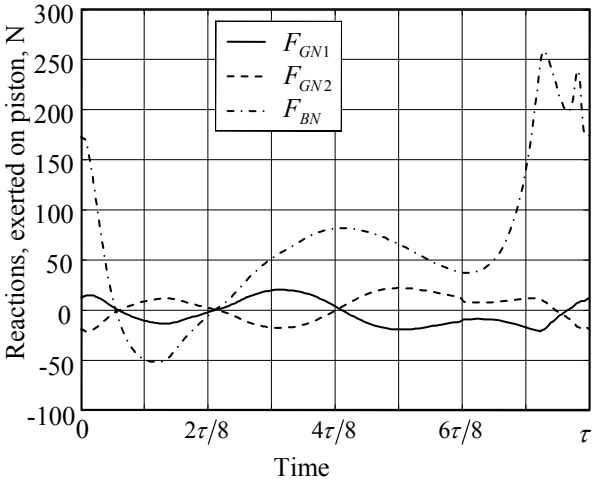

Fig. 7 Reactions, exerted on piston; $\tau = 20.538$ ms

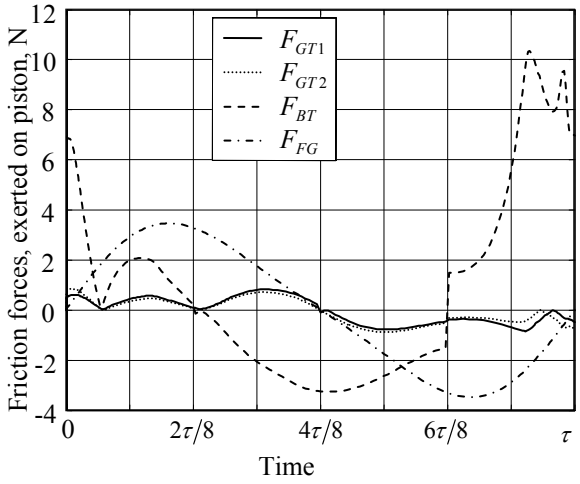

Fig. 8 Friction forces, exerted on piston; $\tau = 20.538$ ms

the bearings with constant relative eccentricity ε, while in our model eccentricity ε is variable. For the case of time dependent film thickness equations for squeeze film should be considered for deeper analysis of the bearings (squeeze films temporary provide increased load capacity). In addition equation (21) in [1] also does not take into account misalignment in the bearings (tilted shaft). Due to high eccentricity ratios as well as cantilever load of crankshaft the centre of hydrodynamic pressure will be shifted towards film thickness, and maximum hydrodynamic pressure will be increased. Due to both these factors maximal values of eccentricity ratios of the bearings (and consequently values of frictional moments) will be decreased. But the main arguments for the use of simplified equation (20) in [1] instead of (21) in [1] can be drawn from the comparison of the average friction power in the bearings (see Fig. 12). Regardless of equation used, the average friction power in the bearings almost does not depend on piston stroke to diameter ratio, piston eccentricity or other compressors parameter, subject to optimisation (except the bearing parameters). Therefore if the model is targeted for overall compressors optimization without particular focus on the bearings, it would be reasonable to consider the use of Eq. (20) in [1] instead of Eq. (21) in [1]. In such case only the first equation of system (1) must be solved at every step of numeric integration instead of the whole system of nonlinear equations, which will reduce calculation which will reduce calculation time significantly.

For heavily loaded bearings Eq. (20) in [1] gives lower integrated friction power, than Eq. (21) in [1]. For analyzed compressor at CECOMAF conditions the difference reached ~20% for M_a and ~10% for M_b. For M_k both equations give similar results (difference ~1%). In absolute values the difference did not exceed 0.7 W, and taking into account the influence of misalignment and squeeze film will further decrease the difference.

Fig. 13 shows friction power in the main friction pairs (power symbol indexes are the same as for corresponding forces). Fig. 14 shows average friction power subject to stroke to diameter ratio. As can be seen, losses for friction in the slider – link friction pair are significant, and can exceed 6 W. The losses in the piston – cylinder friction pair does also exceed 6 W, mainly because of the losses due to the friction force in fluid film. High losses for friction in the slider – link pair is important disadvantage of slider-link driven compressor, if compared to connecting rod driven compressors. However, the overall difference between two types of compressors is lower, than losses in slider – link pair because losses for friction in a connecting rod and pin pair also must be taken into account. Losses in the piston – cylinder pair of connecting rod driven compressor are estimated in [7] and [8] using advansed mathematical models, but direct comparison is complicated due to different geometric, dynamic and op-

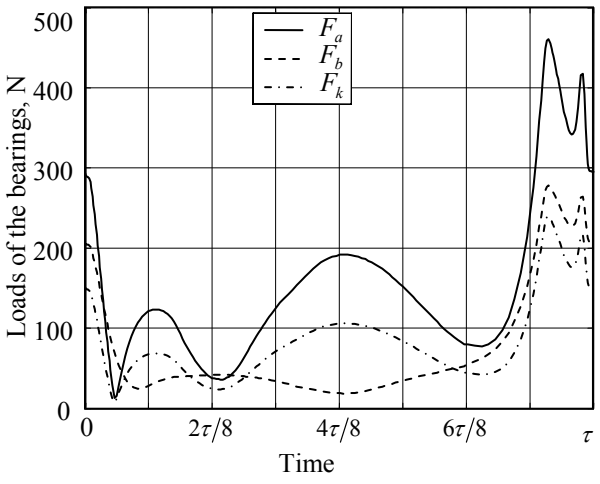

Fig. 9 Loads of the bearings; $\tau = 20.538$ ms

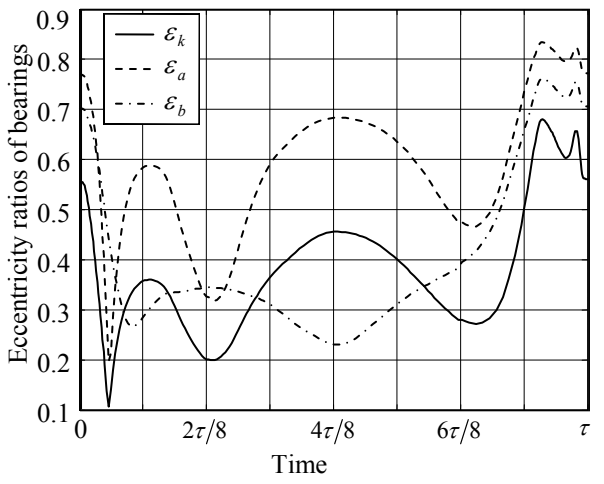

Fig. 10 Eccentricity ratios of the bearings; $\tau = 20.538$ ms

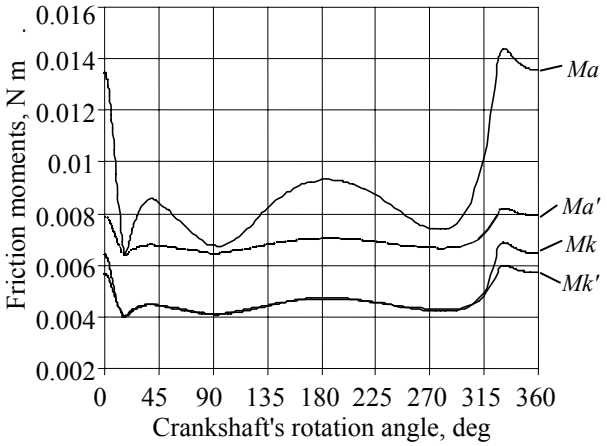

Fig. 11 Frictional moments in a bearings; M_a, M_k calculated using Eq. (21) in [1] and M_a', M_k' calculated using Eq. (20) in [1]

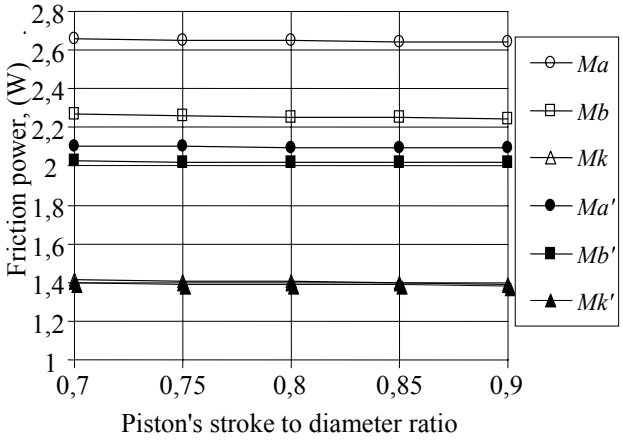

Fig. 12 Average friction power in bearings; M_a, M_b, M_k calculated using Eq. (21) in [1], M_a', M_b', M_k' calculated using Eq. (20) in [1]

erational parameters, used in the simulation. When we used in our model the same piston stroke, diameter, clearance in the piston – cylinder pair and oil viscosity as were used in [7], the estimated average loses for friction in a fluid film were similar - 2 W according to our model and ~2.6 W according to [7]. It is also evident, that some underestimation in our case occurs due to the simplification (misalignment in the friction pair was not taken into account). In the real compressors, however, the picture may be a bit different. In connecting rod driven compressor we will have to use smaller clearance in order to have the same losses because of the leak between the piston and the cylinder, which will increase losses due to friction. Thus overall difference in friction power of two compressor types should not exceed 3 – 5 W (for the same conditions).

The primary goal of the study was to find such set of compressors dimensions that ensures optimum performance of the compressor based on the design criteria. We intended to use design criteria of minimal mechanical losses which was successfully used in [9] for optimization of rotary compressor. The [9] study suggests that more than 50% reduction in a mechanical loss is possible through a proper combination of design dimensions for rotary compressor. This gives an overall improvement of COP (coefficient of performance) of 14%, as the shaft input reduces due to lower frictional losses. However, we failed to get similar results for slider-link driven compressor. As can be seen on Fig. 12, the losses due to friction do decrease as stroke to diameter ratio decreases. This does not necessarily mean that compressor's COP will increase - with increase of the piston diameter, the dead volume will increase, and losses due to leak through the clearance between the piston and the cylinder will increase also. These factors were not taken into account in this study. It is evident, that the attempts to optimize piston stroke to diameter ratio based just on the analysis of friction power does not give satisfactory results. For optimization of this parameter more advanced mathematical model is required, taking into account losses due to the leak through the clearance between the piston and the cylinder.

The model was also used to analyze the impact of piston eccentricity e. Fig. 15 shows the relationship of total friction power subject to piston eccentricity e and piston stroke to diameter ratio. Calculations prove the existence of optimal piston eccentricity - with increase of compressors volume from $V = 5\,\text{cm}^3$ to $V = 9\,\text{cm}^3$, optimal eccentricity increases from $3.7\,\text{mm}$ to $4.8\,\text{mm}$ for ratio $S/D = 0.8$. However, the influence of this parameter is fairy small and theoretical gain from such optimization will not exceed 0.5 W.

The mathematical model can be also used for the

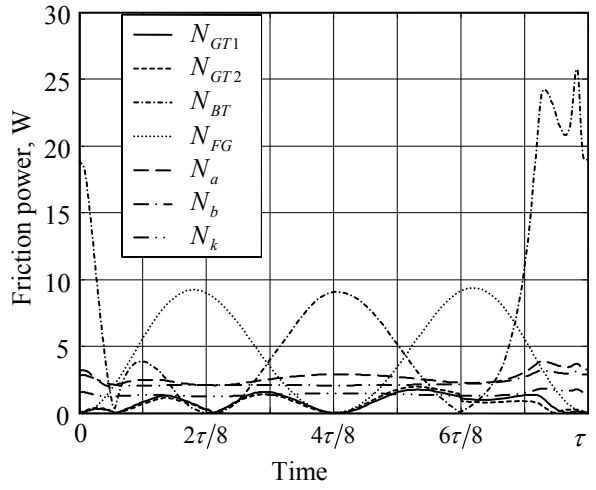

Fig. 13 Friction power in the main friction pairs; $\tau = 20.538$ ms

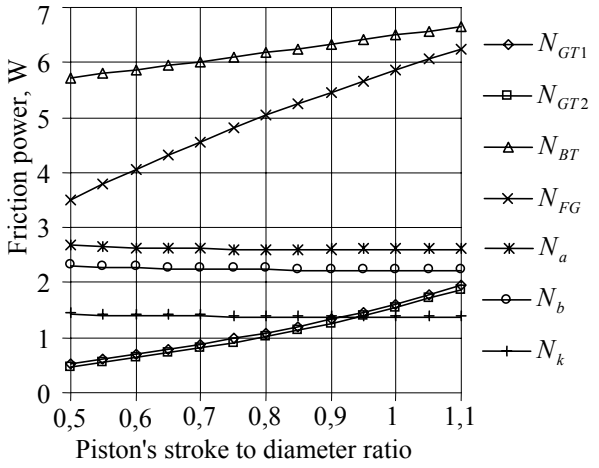

Fig. 14 Average friction power; $V = 9.55\ \text{cm}^3$, $t_c = 40\,^{\circ}\text{C}$, $t_o = -23.3\,^{\circ}\text{C}$

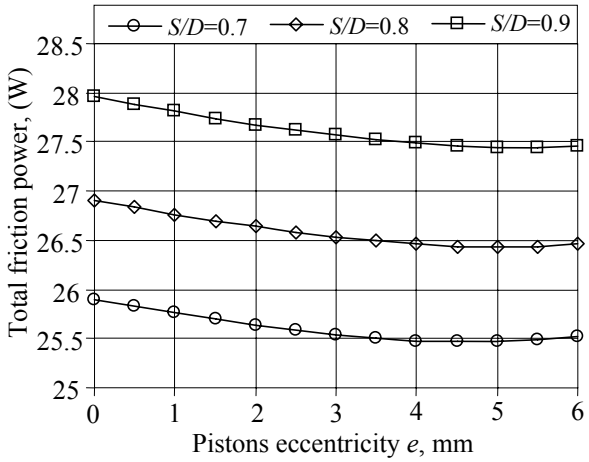

Fig. 15 Total friction power subject to pistons eccentricity e and pistons stroke to diameter ratio S/D; $V = 9.55\,\text{cm}^3$, $t_c = 40\,^\circ\text{C}$, $t_o = -23.3\,^\circ\text{C}$

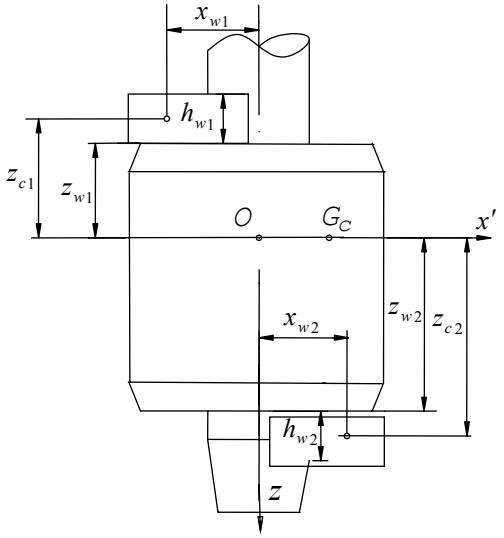

Fig. 16 Variables, used for calculation of counterweights

evaluation and minimization of inertia forces. The unbalanced inertia forces and moments of forces can be minimized by the use of two counterweights. The counterweights are selected to satisfy the following conditions

$$\left(F_x\right)_{max} = \left(F_y\right)_{max},\ \left(M_x\right)_{max} = \left(M_y\right)_{max} \qquad (3)$$

where $\left(F_x\right)_{max}$, $\left(F_y\right)_{max}$ are peak values of the components of resultant inertia force; $\left(M_x\right)_{max}$, $\left(M_y\right)_{max}$ are peak values of the moments of resultant inertia force. The peak values can be found from equations (40) in [1] after the equation of rotating motion of the crankshaft (35) in [1] is solved.

The coordinates of counterweights mass centers in z direction are $z_{c1} = z_{w1} - |h_{w1}|/2$, $z_{c2} = z_{w2} + |h_{w2}|/2$ where z_{w1}, z_{w2} are distances from mass center of the compressor to counterweights mounting planes (see Fig.16); h_{w1}, h_{w2} are heights of upper and lower counterweights. The positive values h_w are assumed for the counterweights, placed as on Fig 16. Negative value of h_w means that the counterweight must be placed on the opposite side relatively the axis of rotation.

The coordinates of counterweights mass centers in x' direction are $x_{w1} = -x_c sign\left(h_{w1}\right)$, $x_{w2} = x_c sign\left(h_{w2}\right)$ where x_c is the distance from the rotation axis to the mass center of a counterweight.

Mass properties of the counterweights are $m_{wi} = m_r |h_{wi}|$; $J_z = J_r\left(|h_{w1}| + |h_{w2}|\right)$; $J_{x'z} = \sum_{i=1}^{2} m_{wi} x_{wi} z_{ci}$ where m_{wi} - counterweight mass with the height h_{wi} $(i = 1,2)$; m_r, J_r - the mass and inertia moment of counterweight with the height 1; J_z - inertia moment of both counterweights with respect to rotation axis; $J_{x'z}$ - product of inertia of counterweights with respect to x', z axes.

To find the heights of counterweights, ensuring minimization of inertia forces, the system of nonlinear equations (3) is solved, with the equation of rotating mo tion of the crankshaft (35)[1] solved at every step. However, the heights of the upper and the lower counterweights h_{w1} and h_{w2} can not be used as independent variables for

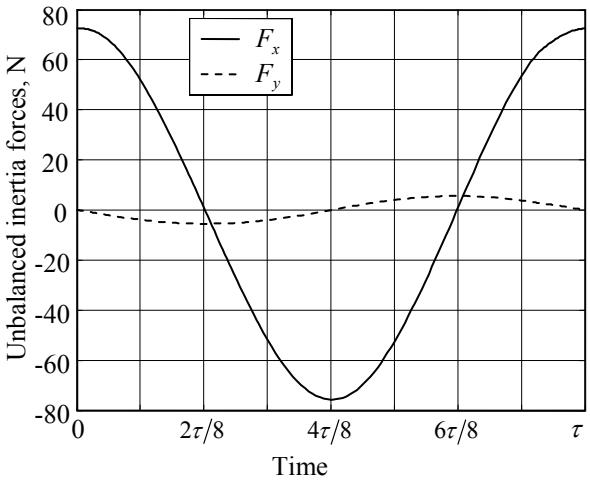

Fig. 17 Unbalanced inertia forces with basic counterweight setup; $h_{w1} = 5\,\text{mm}$, $h_{w2} = 0$, $\tau = 20.538$ ms

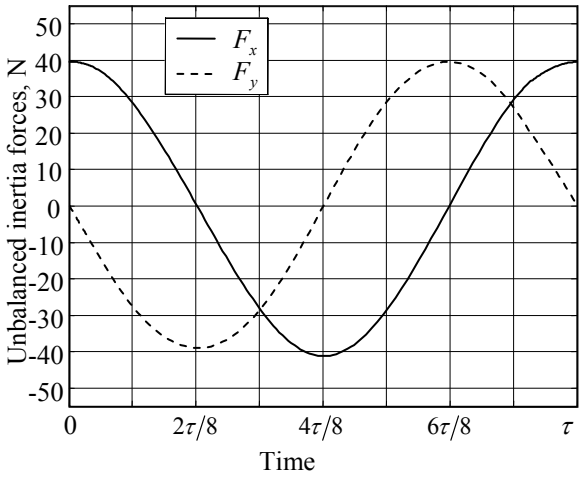

Fig. 18 Unbalanced inertia forces with optimized counterweights; $h_{w1} = 15.0\,\text{mm}$, $h_{w2} = 5.4$, $\tau = 20.537$ ms

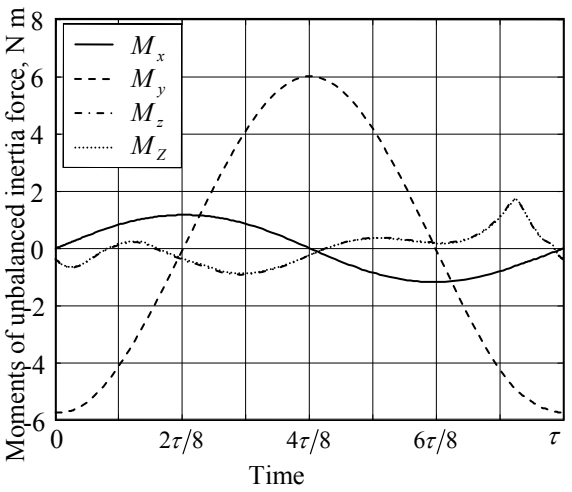

Fig. 19 Moments of unbalanced inertia forces with basic counterweight setup; $h_{w1} = 5\,\text{mm}$, $h_{w2} = 0$, $\tau = 20.538$ ms

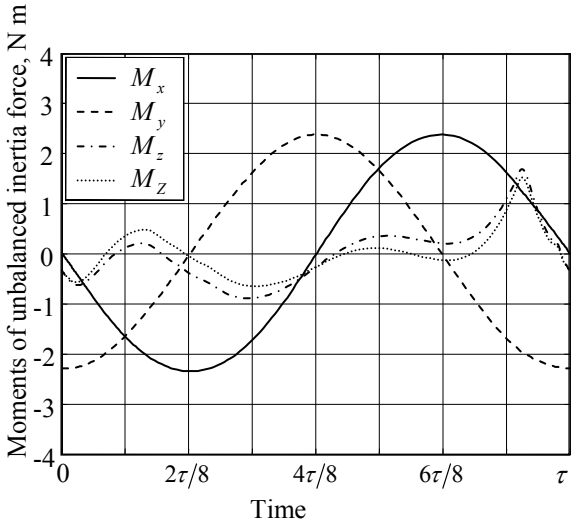

Fig. 20 Moments of unbalanced inertia forces with optimized counterweights; $h_{w1} = 15.0\,\text{mm}$, $h_{w2} = 5.4$, $\tau = 20.537$ ms

solving the nonlinear system of equations (3) as the algorithm does not converge to the solution. Possible workaround is to use as independent variables the height of counterweight for static balancing h_1 and the height of pair of counterweights for dynamic balancing h_2. If the counterweight for static balancing is placed only on upper end of the rotor, and the pair of counterweights for dynamic balancing is placed on both ends, heights of upper and lower counterweights can be calculated as $h_{w1} = h_1 + h_2$; $h_{w1} = h_2$.

Figs. 17 and 19 shows unbalanced inertia forces and moments of the forces with basic counterweight setup while Figs. 18 and 20 shows the forces and the moments with optimized counterweights. Peak values of the forces and the moments with optimized coun terweights decreased by almost 50%. A compressor with such counterweight setup was tested in a refrigerator. Noise level of the refrigerator decreased by almost 2 dB.

Implementation of such counterweight setup would be quite complicated – higher counterweights require additional space, which is not always available. However, such height of counterweights is required only for compressors with bigger volume and piston diameter $D = 26$ mm. Slider – link driven compressors with such piston diameters will face also other technical challenges, such as significant deformation of the cylinder during bolt tightening. The problems can be solved with deeper compressor redesign, but such path is not very practical because of required investments. On the other hand, in the modern refrigerators a trend for increased use of lower capacity compressors can be observed, and the demand for compressors with such extreme diameters will decrease.

As mentioned above, the advantage of connecting rod driven compressor over slider - link driven compressor is not that big (estimated difference 3-4 W) when friction power is considered. Evolutionary transition from slider – link driven compressor to connecting rod driven compressor is close to impossible. It requires major redesign and the change of almost all manufacturing equipment. Probably the only alternative for such transition would be the use of spherical joint between the piston and connecting rod. Such joint could be considered as a means to avoid extreme piston diameter (especially if such compressors are manufactured in small series).

On the other hand, the really impressive compressor efficiency growth, demonstrated recently by leading manufacturers, was reached mainly by means of motor efficiency increase. Therefore remaining manufacturers of "outdated" slider-link driven compressors (usually the small ones with tight budget) should concentrate their resources on acquirement and implementation of high efficiency motor, with only the limited scale optimization of existing designs of compressor itself. With modern motors the COP of 1.6-1.66 (at ASHRAE test conditions) for slider link driven compressor is not out of reach. Such efficiency usually is enough to ensure A and even A+ energy efficiency class of modern refrigerators.

3. Conclusions

The mathematical model, described in this paper, can be used for the calculation of forces and dynamic behaviour of slider-link driven compressor. Calculated relationship of crankshaft speed subject to evaporation temperature is very close to the measured values (difference ~0.2%).

Losses for friction in the slider–link pair is a disadvantage of slider-link driven compressor. However, for the same dimensions and operation conditions overall difference in friction power (when compared to connecting rod driven compressor) should not exceed 3 – 5 W.

Attempts to optimize piston stroke to diameter ratio based just on the analysis of friction power does not does not give satisfactory results. Optimization of piston stroke to diameter ratio requires more advanced mathematical model, in which losses due to leak between the piston and the cylinder would be taken into account. The design criteria for such optimization should be maximal COP.

Optimal pistons eccentricity based on design criteria of minimal mechanical losses does exist, but positive effect from such optimization is minimal - theoretical gain will not exceed 0.5 W.

Slider – link driven compressor still has some potential for modernization, especially when smaller capacity range is considered. For small manufacturers limited scale optimization together with the implementation of high efficiency motors will be more cost-effective solution than transition to connecting rod driven compressors.

If the model is targeted for overall compressor optimization without particular focus on slider bearings, it would be reasonable to use consider use equation (20) in [1] instead of (21) in [1]. For optimization of the bearings the improved model should be developed in which misalignment (tilted shaft) and squeeze film should be taken into account.

References

1. **Dagilis, V., Vaitkus, L., Kirejchick, D.** Slider-link driven compressor (I). Mathematical model. -Mechanika. -Kaunas: Technologija 2006; Nr.6(62), p.25-31.
2. **Vaitkus, L.** Research and simulation of valve system of hermetic refrigerating compressor.-Doctoral thesis. -Kaunas, 1998.-108p. (in Lithuanian).
3. **Dagilis, V., Vaitkus, L.** Research of the gas flow through the irregular clearance.-Mechanika.-Kaunas: Technologija, 1997, Nr.2(9), p.18-21.
4. **Imaichi, K., Fukushima, M., Muramatsu, S., Ishii, N.** Vibration analysis of rotary compressors.-Proc. of the Int. Compressors Engineering Conf. at Purdue. - USA, 1984, p.275-282.
5. **Ooi, K.T., Wong, T.N.** A computer simulation of a rotary compressor for household refrigerators.-Appied Thermal Engineering, 1997, No.1, v.17, p.65-78.
6. **Rigola J.S.** Numerical simulation and experimental validation of hermetic reciprocating compressors. Integration in vapour compression refrigerating systems. -Doctoral thesis.-Terrassa, 2002.-109p.
7. **Prata, A.T., Fernandes, J.R.S., Fagotti, F.** Dynamic analysis of pistons secondary motion for small reciprocating compressors.-J. of Tribology: ACME, 2000, v.122/753, p.752-760.
8. **Cho, J.R., Moon, S.J.** A numerical analysis of the interaction between the piston oil film and the component deformation in a reciprocating compressor.-J. of Tribology.-ELSEVIER, 2005, v.38, Issue 5, p.459-468.
9. **Ooi, K.T., Wong, T.N.** Design optimization of a rolling piston compressor for refrigerators.-Appied Thermal Engineering, 2005, v.25, p.813-829.

V. Dagilis, L. Vaitkus, D. Kirejchick

KULISINIS KOMPRESORIUS (II). MODELIAVIMO REZULTATAI

R e z i u m ė

Kulisinio komresoriaus modelis panaudotas skaičiuojant judančių mechanizmo dalių dinamiką, reakcijas, trinties jėgas ir neišsvertas inercijos jėgas. Modeliavimo rezultatai palyginti su pamatuotomis sukimosi greičio reikšmėmis, matuotos ir skaičiuotos reikšmės gerai sutapo. Modelis naudojamas analizuojant, kaip kompresoriaus darbą įtakoja įvairūs jo parametrai, tokie kaip stūmoklio eigos ir diametro santykis, stūmoklio ekscentricitetas, cilidro tūris. Bandymas optimizuoti kompresoriaus parametrus remiantis minimalių mechaninių nuostolių kriterijumi nedavė norimų rezultatų. Bendrai kompresoriaus optimizacijai turi būti sukurtas modelis, tiksliau charakterizuojantis kompresoriaus termodinaminius procesus.

V. Dagilis, L. Vaitkus, D. Kirejchick

SLIDER-LINK DRIVEN COMPRESSOR (II). SIMULATION RESULTS

S u m m a r y

The model of slider-link driven compressor is used to calculate dynamic behaviour of movable machine elements, constraint forces, friction forces, unbalanced inertia forces. Simulation results were compared to experimental measurements of rotation speed, good agreement between numerical and experimental data was obtained. The model is used for analysing the influence of various parameters, such as piston eccentricity, piston stroke to diameter ratio, displacement on compressors performance. The attempt to performe optimization of compressor parameters based on criterion of minimal mechanical losses does not give satisfactory results. The model with more detailed thermodynamic characterization of the compressor should be developed for overall compressor optimization.

В. Дагилис, Л. Вайткус, Д. Кирейчик

КУЛИСНЫЙ КОМПРЕССОР (II). РЕЗУЛЬТАТЫ МОДЕЛИРОВАНИЯ

Р е з ю м е

Модель компрессора с кулисным приводом применяется для расчета динамики подвижных частей, реакций, сил трения и неуравновешенных сил инерции. Результаты моделирования сравниваются с экспериментальными данными, получена хорошая сходимость расчетных и экспериментальных результатов. Модель используется для анализа влияния на работу компрессора разных параметров, таких как эксцентриситет поршня, отношения хода поршня к диаметру, объем цилиндра. Попытка оптимизации параметров компрессора, основана на минимизации механических потерь, не дала желанного результата. Для общей оптимизации компрессора должна быть разработана математическая модель, более точно отражающая термодинамические процессы компрессора.

Received September 04, 2006